Experimental and Numerical Investigation of a Cracked Cantilever Beam for Damping Factor to Access its Applicability in the Crack Detection

V. Khalkar[1], S. G. Kumbhar[2], K. Logesh[3], P. Hariharasakhtisudhan[4], S. D. Jadhav[5], B. A. Danawade[6], S. H. Gharat[7], L. M. Jugulkar[8], J. G. Borade[9]

[1]Department of Mechanical Engineering, Gharda Institute of Technology, Lavel, Khed, Ratnagiri, India (vikas_khalkar@rediffmail.com); [2]Department of Automobile Engineering, Rajarambapu Institute of Technology, Islampur, Sangli, India (surajkumar.kumbhar@ritindia.edu); [3]Department of Mechanical Engineering, Vel Tech Rangarajan Dr. Sagunthala R&D Institute of Science and Technology, Chennai, India (klogesh7@gmail.com); [4]Department of Mechanical Engineering, National Engineering College, Kovilpatti, India (harimeed2012@gmail.com); [5]Department of Mechanical Engineering, Bharati Vidyapeeth College of Engineering, Navi Mumbai, Mumbai, India (sandhya.jadhav@bhartividyapeeth.edu); [6]Department of Mechanical Engineering, Gharda Institute of Technology, Lavel, Khed, Ratnagiri, India (badanawade@git-india.edu.in); [7]Department of Chemical Engineering, Gharda Institute of Technology, Lavel, Khed, Ratnagiri, India (shgharat@git-india.edu.in); [8]Department of Automobile Engineering, Rajarambapu Institute of Technology, Islampur, Sangli, India (lalitkumar.jugulkar@ritindia.edu); [9]Department of Computer Engineering, Gharda Institute of Technology, Lavel, Khed, Ratnagiri, India (jvkhalkar@git-india.edu.in)

Abstract

The cracks alter the physical and modal properties of the beam, i.e., stiffness, damping, natural frequency, and mode shapes, and, in turn, the dynamic response of the beam changes to a considerable extent. The condition monitoring of the beams is essential to avoid its catastrophic failure in applications. A basic criterion has been followed for modal parameters like natural frequencies, mode shapes, and stiffness for the possible crack detection. In contrast, damping as a dynamic property to represent structural damage has been limited due to the difficulties in measuring damping and analysis. Therefore, in this study, the effect of various possible crack profiles, i.e., V-shaped and U-shaped, on the applicability of using the damping criterion for determining the presence of damage in the cantilever structure was investigated. The damping loss factor for all the cracked cases of a cantilever beam was computed using ANSYS and experimental analysis. The numerical results of the damping loss factor were compared with experimental results. It was understood that the results were susceptible to the crack geometries changes.

Author Keywords. Effective Mass, Dewesoft FRF, Impact Hammer, V-shaped Crack, U-shaped Crack, Structural Health Monitoring, ANSYS, Torsional Stiffness, Resonant Amplitude.

Type: Research Article

1. Introduction

A structural health monitoring system is generally designed to monitor, inspect and test the health and performance of structures such as beams, buildings, bridges, and dams, to ensure their safety. It mainly consists of two major components: the smart sensing technologies and the damage detection algorithms. The smart sensing technologies use fiber optic sensors, piezoelectric sensors, laser Doppler vibrometers, and accelerometers to monitor various

physical responses of the structures or any set-up under investigation. The damage detection algorithms reveal the damage characteristics from the responses measured by smart sensing sensors.

Bayissa, Haritos, and Thelandersson (2008) developed a new damage identification technique based on the statistical moments of the energy density function of the vibration responses in the time–frequency domain. Using the continuous wavelet transform, they decomposed the vibration responses into discrete energy distributions as a joint function. Then, they extracted the principal structural response features from the energy density functions using the moments. The zero*th*-order moment known as the total energy of the joint density function was then computed at each measurement grid point for the pre-damage and post-damage states and then implemented for detection and localization of damage in a concrete plate model in a steel plate girder of a bridge structure. Curadelli et al. (2008) presented the novel scheme to detect structural damage by identifying an instantaneous damping coefficient using a wavelet transform. The laboratory tests and the numerical simulations exhibited significant changes in the damping characteristics of commonly used structural systems. Therefore, it was ensured that the parameters, which characterize the structural damping, could be used as a damage-sensitive system property. Frizzarin et al. (2010) developed the baseline free, time domain damage detection method for concrete structures. The method was based on the analyzing nonlinear damping from the measured structural vibration responses. The effectiveness of the proposed method was verified through a large-scale concrete bridge model subjected to different levels of seismic damage caused by the shaking table tests. The nonlinear damping was increased with respect to the seismic damage. Kawiecki (2001) studied the application of arrays of surface-bonded piezo elements to determine the modal damping characteristics of a tested structure, and the damping characteristics were then used for detecting the structural damage. Khalkar and Ramachandran (2017a, 2018a, 2019) studied the dynamic behavior of a cracked beam. They have covered several aspects, including the effect of crack geometry and crack location on the dynamic behavior of structures. They also emphasized the damage quantification and the implementation of existing mathematical models to assess the dynamic behavior of structures with various crack geometries. Kyriazoglou, Le Page, and Guild (2004) expressed that the measurement of specific damping capacity (SDC) was a proper potential method for detecting damage. In this study, the measurement and analysis of SDC of composite beams in flexure were carried out using quasi-static loading or fatigue, and beams were tested before and after the introduction of damage. The results of this study indicated that the measurement of SDC was a promising technique for detecting initial damage in woven fabric composites. Razak and Choi (2001) conducted an experimental investigation to study the effect of general corrosion on the modal parameters of reinforced concrete beams. The states of damage in the test beams were measured by measuring crack width and spalling. Modal tests were performed on the test beams after corrosion damage, and the extracted modal parameters were compared against the control beam. The obtained results showed the considerable changes in the natural frequencies and damping ratio. Orhan et al. (2016) introduced the new crack model (combination of V-shaped and rectangular-shaped crack). They investigated the effect of crack depth on the natural frequency of a composite beam.

From the literature survey, it was found that limited research works have been carried out on the damping-based crack detection method in the condition monitoring of structures. The damage detection is a vital phenomenon for allowing wider use of composite laminates in critical applications. Furthermore, the damping characteristics are frequently associated with

the structural as well as material damage. In this research work, it was decided to check the applicability of the damping-based damage detection technique in the cracked structure. The damping loss factor in the cracked structures was obtained using experimental and numerical methods. The analysis was extended for different profiles of cracks artificially induced in the cantilever structure at different locations from the fixed end. The crack depths were also varied to investigate the effect of damping in damage detection.

2. Theoretical Analysis

2.1. Stiffness model of a cracked beam

In this research study, V-shaped and U-shaped cracks (Khalkar and Ramachandran 2018b) were considered on the cantilever beam to study the effect of shape of the crack on the modal properties of the beams. Figure 1 and Figure 2 show the configurations of a cantilever beam with V-shaped and U-shaped cracks. When a beam carries a crack at any location, then the two segments of the beam on either sides of the crack can be assumed to be connected by the torsional spring, as shown in Figure 3. The torsional stiffness (Khalkar and Ramachandran 2019) of a cracked beam was calculated using Equation (1).
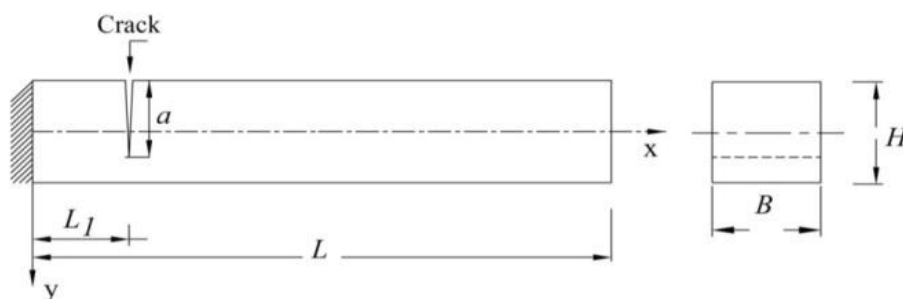

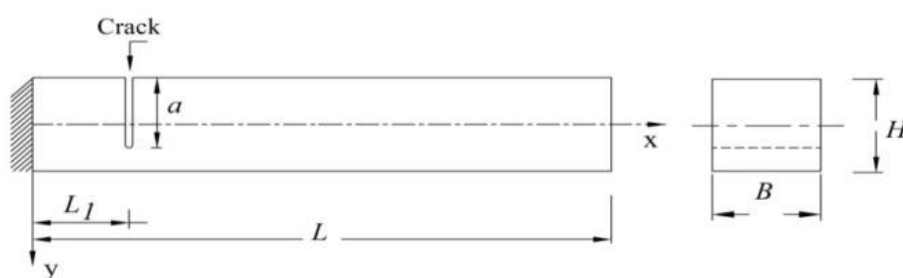**Figure 1**: A cracked cantilever beam with a V-shaped crack

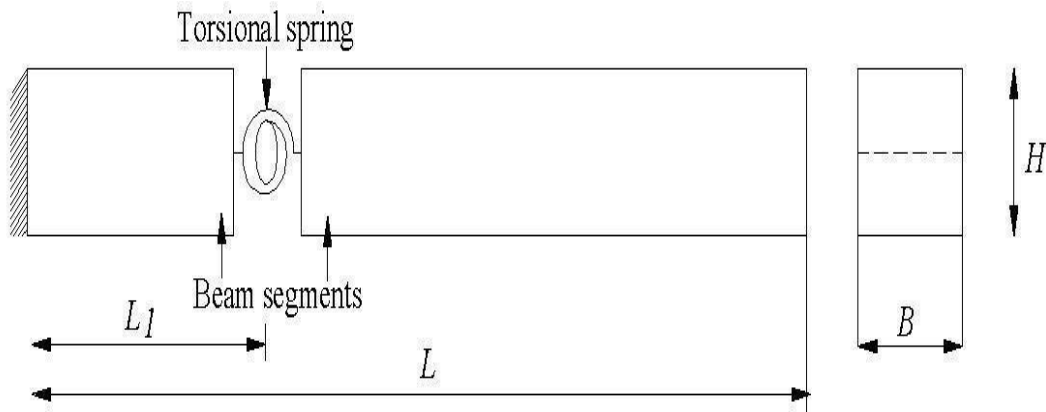**Figure 2**: A cracked cantilever beam with a U-shaped crack

Figure 3: Stiffness model of a cracked cantilever beam

$$K_T = \frac{EBH^2}{72\pi(L - L_1)^2\,(1 - \mu^2)\Phi} \tag{1}$$

The Φ is the variable and it is the function of crack depth ratio (a/H); and it is given by

$$\Phi = 0.629\left(\frac{a}{H}\right)^2 - 1.047\left(\frac{a}{H}\right)^3 + 4.602\left(\frac{a}{H}\right)^4 - 9.975\left(\frac{a}{H}\right)^5 + 20.295\left(\frac{a}{H}\right)^6 - 32.993\left(\frac{a}{H}\right)^7$$
$$+ 47.041\left(\frac{a}{H}\right)^8 - 40.693\left(\frac{a}{H}\right)^9 + 19.6\left(\frac{a}{H}\right)^{10} \tag{2}$$

Hence, the equivalent stiffness of the open-edge cracked beam (k) was computed using Equation (3).

$$k = \frac{K_T K_I}{K_T + K_I} \tag{3}$$

The stiffness of an intact or un-cracked cantilever beam (K_I) was computed using Equation (4), where E, I and L are the Young's modulus, mass moment of inertia and length of the cantilevered beam respectively. The torsional stiffness and open-edged cracked beam for various cracked cases are presented in Table 3 and Table 4, respectively.

$$K_I = \frac{3EI}{L^3} \tag{4}$$

2.2. Modeling of a cracked cantilever beam as a discrete system

The transverse vibration of an open-edge cracked cantilever beam was modeled as a single-degree of freedom system. An equivalent single-degree freedom (Thomson and Dahleh 1998) system model is shown in Figure 4. When the cantilever beam vibrates with first natural frequency, it gives the fundamental bending mode. For this reason, the first fundamental mode of a cracked cantilever beam was predominantly excited; to get the resonance amplitude. The magnification factor ($\frac{X}{X_{st}}$) of the vibrating beam is independent of the harmonic force; hence, 50 N harmonic forces were selected and applied at the free end of the cracked cantilever beam.
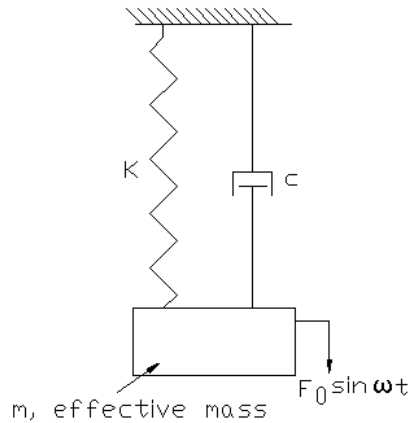
Figure 4: A cracked cantilever beam modeled as a spring mass damper system with harmonic force

The free-body diagram for the spring-mass damper system, based on Newton's law of motion, is shown in Figure 5. The fundamental equation of motion is given in Equation (5).
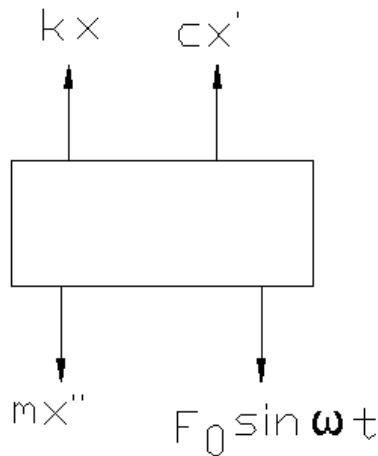

Figure 5: A Free body diagram of a cracked cantilever beam

$$m\ddot{x} + c\dot{x} + kx = F_0 \sin\omega t \tag{5}$$

The solution to Equation (5) consists of two parts, i.e., complementary function and particular integral. In this study, the attention was given to the second part, i.e., forced vibration. When a system is subjected to harmonic excitation, it is forced to vibrate at the same frequency as excitation.

Assume the particular integral solution of Equation (5) to be in the form of Equation (6).

$$x = X\sin(\omega t - \Phi') \tag{6}$$

where, X is the amplitude of oscillation and Φ' is the phase of the displacement concerning excitation force.

The amplitude of vibration was found by substituting the value of Equation (6) in Equation (5).

$$X = F_0 / \sqrt{(k - m\omega^2)^2 + (c\omega)^2} \tag{7}$$

Dividing numerator and denominator of Equation (7) by k

$$X = \frac{\frac{F_0}{k}}{\sqrt{\left(1 - \frac{m\omega^2}{k}\right)^2 + \left(\frac{c\omega}{k}\right)^2}} \tag{8}$$

Equation (8) can be expressed in the following terms:

$$c_c = 2m\omega_n$$

$$\zeta = c/c_c$$

$$\frac{c\omega}{k} = 2\zeta\,\omega/\omega_n$$

Equation (7) can be rewritten as follows:

$$X = \frac{\frac{F_0}{k}}{\sqrt{\left[1 - \left(\frac{\omega}{\omega_n}\right)^2\right]^2 + [\,2\zeta\,\omega/\omega_n]^2}} \tag{9}$$

But, $\frac{F_0}{k} = X_{st}$, where X_{st} is the zero frequency deflection.

The ratio between steady state amplitude (X) and zero frequency deflection (X$_{st}$) is called as magnification factor

At resonance, $\omega = \omega_n$, and $X = X_{res}$, hence Equation (8) becomes

$$X_{res} = \frac{\frac{F_0}{k}}{2\zeta} \tag{10}$$

$$\therefore\ \zeta = \frac{\frac{F_0}{k}}{2X_{res}} \tag{11}$$

Thus, the damping loss factor of each cracked case is obtained by substituting the value of open-edge cracked beam stiffness and resonant amplitude in Equation (11). The numerical damping loss factors of all the cracked cases are presented in Table 6.

3. Simulated Crack Configurations

Geometric properties: The geometric properties of the cantilever beam are presented in Table 1. The material of the cantilever beam was EN 42. The properties of EN 42, i.e., Modulus of elasticity and Density, were tested in ELCA Lab, Pune, India and are presented in Table 2.

Length (m)	Width (m)	Depth (m)
0.5	0.02	0.02

Table 1: Geometric properties of a cantilever beam

Property	Euro Norm 42
Young's modulus (N/m²)	2.0549 x 10¹¹
Mass density (kg/m³)	7840
Mass (kg)	1.568
Effective mass (kg)	0.3695

Table 2: Material properties of EN 42 cantilever beam

In the present study, a total of 24 cracked specimens were considered to investigate the effect of the different profiles of cracks on the stiffness and modal damping loss factor of a cantilever beam. Two separate cases were considered as case 1 and case 2.

Case 1: In this case, 12 specimens with V-shaped cracks induced in the cross-section were considered. Out of 12 specimens, three specimens contained cracks at a distance of 100 mm from the fixed end. Then, three specimens carried cracks at the distance of 200 mm, and three more specimens possessed cracks at 300 mm from the fixed end. The remaining three specimens were considered with cracks at 400 mm from the cantilevered end. At all these locations, the crack depth was varied from 5 mm to 15 mm by an interval of 5 mm.

Case 2: The location of the cracks and depth of the cracks are similar to case 1; the only difference is that instead of V-shaped cracks, U-shaped cracks were considered in the beams.

4. Numerical Modeling

ANSYS 12.1 finite element program was used to determine the cracked cantilever beams' zero-frequency deflection and resonant amplitude. The zero-frequency deflection of a three-dimensional cracked beam was obtained through a typical procedure. First, a rectangular area of required geometric properties was created and then extruded to create the three-dimensional model. The crack was modeled by creating a small volume model at the required location in the primary model. The crack volume was then subtracted from the volume of the primary model. The finite element model of the cracked beam was obtained using a solid 186 element. A static load of 50 N was applied at the free end of the cantilever beam to get the zero-frequency deflection (Khalkar and Ramachandran 2017b). The stiffness of a cracked beam was determined using the conventional formula, i.e., Stiffness= Load/Deflection. The one case of a cracked cantilever beam carrying a static load at the free end is shown in Figure 6. From Figure 6, it is clear that the cantilever beam has a crack at the location where the mesh type is irregular. The stiffness results for various cracked cases are presented in Table 4. In this study, the difference between the total mass of an intact beam (M) and the cracked beam (m) with the most considerable crack depth was negligibly small. Hence, for all the cracked cases, the total mass of an intact beam was considered the total mass of cracked beams, i.e., $M = m$. When the cantilevered beam vibrates in the first bending mode, the only effective mass of the beam comes into the picture and leads to producing the vibration. In this research study, the effective mass of a cracked cantilever beam (Khalkar and Ramachandran 2017a) was chosen as, i.e., $m_{eff} = 0.2357M$. The effective mass (m_{eff}) of an intact cantilever beam or cracked cantilever beam is presented in Table 2. The effective mass was considered to find the resonant amplitude of the cracked cantilever beams. The mass 21-point element and combination 14 elements were used to model a discrete model in ANSYS. A harmonic force of 50 N was applied to discrete system to obtain the displacement response of the system. In harmonic analysis, the frequency sweep of zero to 80 Hz was selected. One case of the equivalent spring-mass-damper system carrying the harmonic force is shown in Figure 7. The resonant amplitude computed for the various cracked cases is presented in Table 5. The one FEA plot of harmonic analysis of a cracked cantilever beam is shown in Figure 8, i.e., amplitude versus excitation frequency.
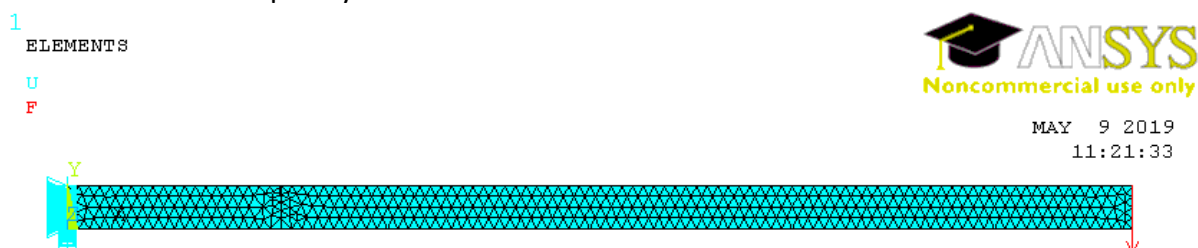

Figure 6: A cracked cantilever beam carries a zero-frequency point load at the free end
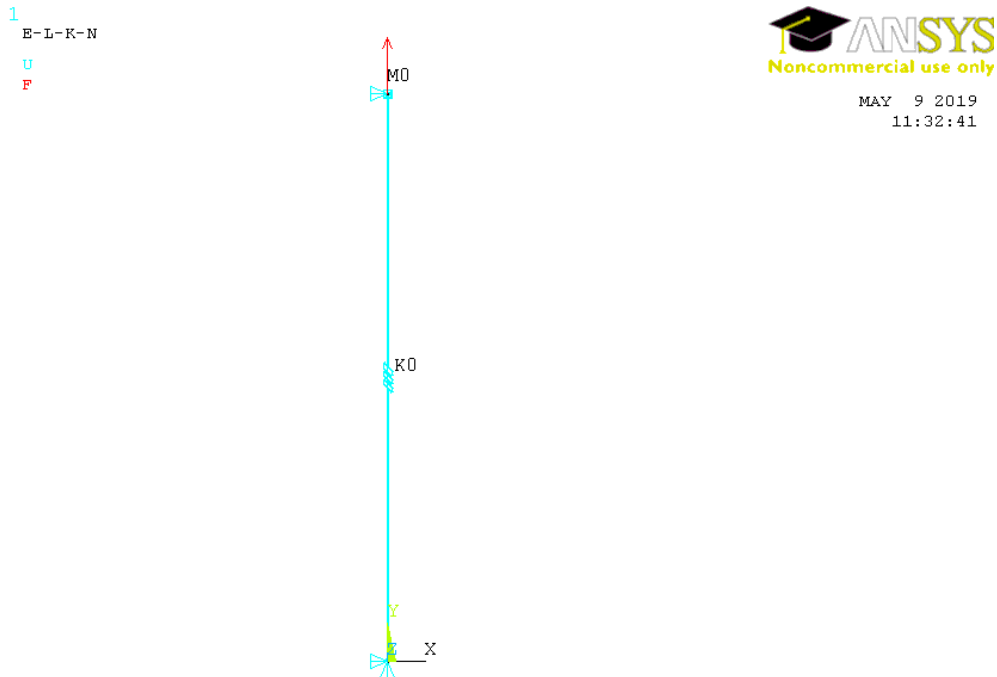
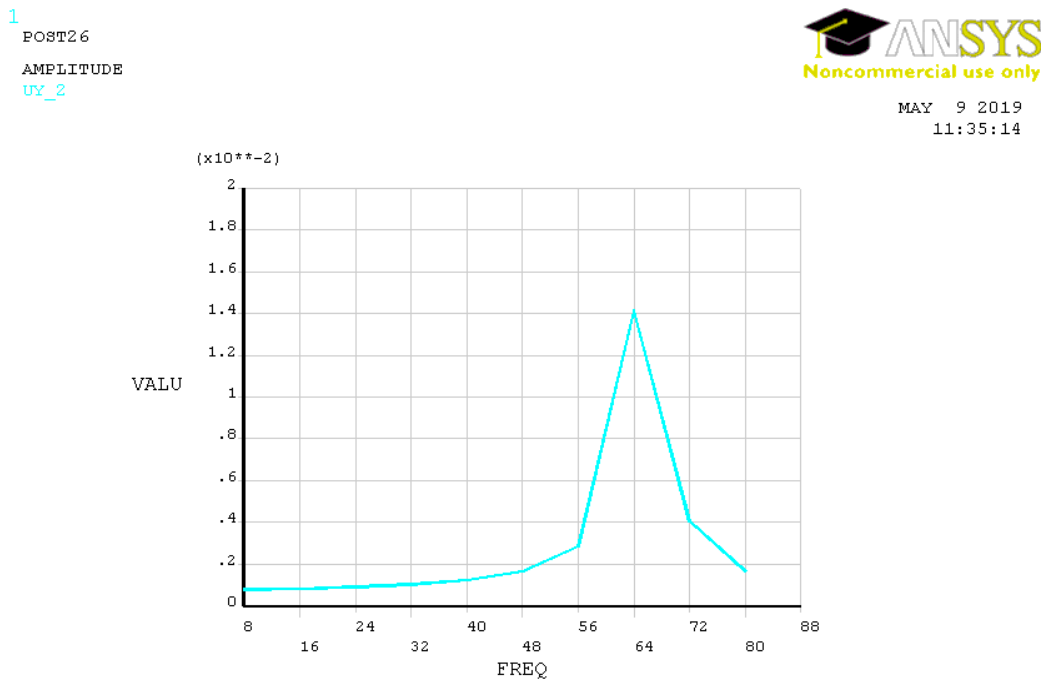**Figure 7**: An equivalent spring-mass-damper model of a cracked cantilever beam subjected to a harmonic force

Figure 8: FEA plot of harmonic analysis of a cracked cantilever beam

5. Experimental Investigation

The main aim of the experimentation is to compute the damping loss factor of cracked cases of the beam. A cantilever beam was machined from EN 42 material. The open-edge V-shaped and U-shaped cracks were produced on the specimens using wire Electro Discharge Machining (EDM). For experimental analysis, i.e., Dewesoft Frequency Response Function (FRF), four-channel Fast Fourier Transform (FFT) analyzer, accelerometer, impact hammer, and related accessories were used. The experimental setup is shown in Figure 9. A disturbance was given on the specimen using the impact hammer to induce the transverse vibration of a cracked

beam. The Dewe-FRF plots of damping loss factors of various cracked cases are shown in Figures 10-13.

Figure 9: Experimental Rig

Figure 10: Damping loss factor of a V-shaped cracked case; Crack location 100 mm; Crack depth 5 mm

Figure 11: Damping loss factor of a U-shaped cracked case; Crack location 100 mm;
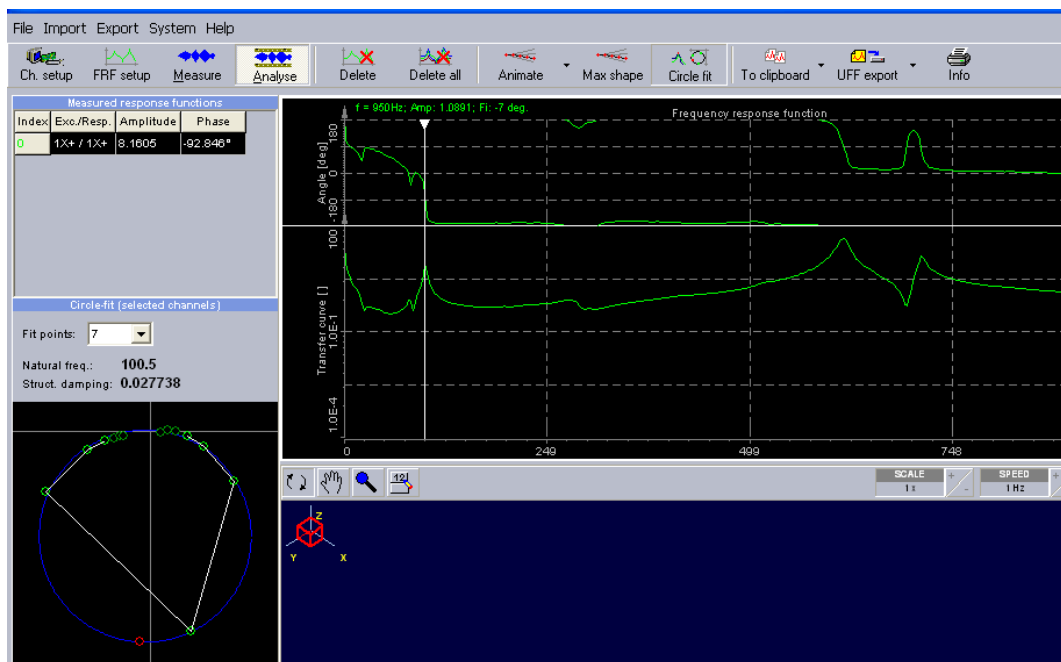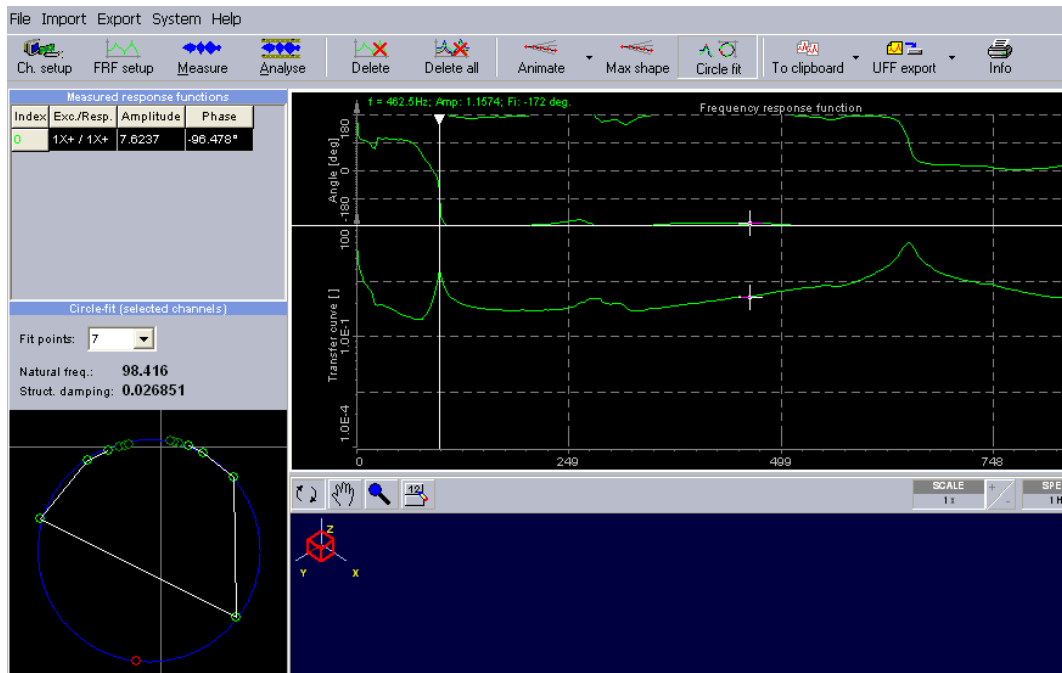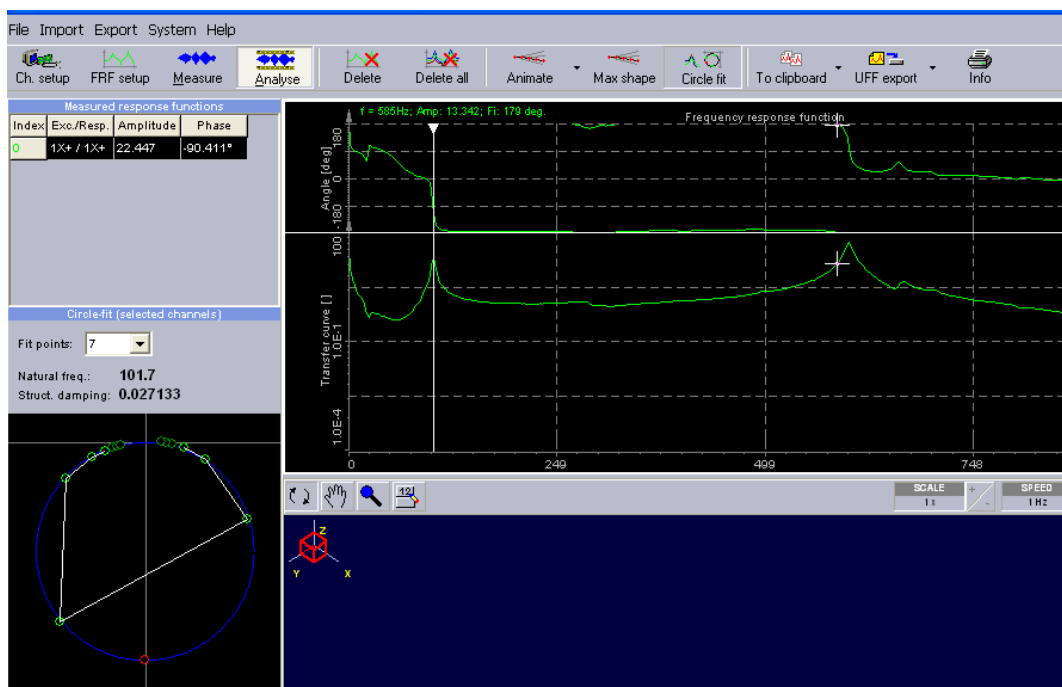Crack depth 5 mm

Figure 12: Damping loss factor of a V-shaped cracked case; Crack location 200 mm;
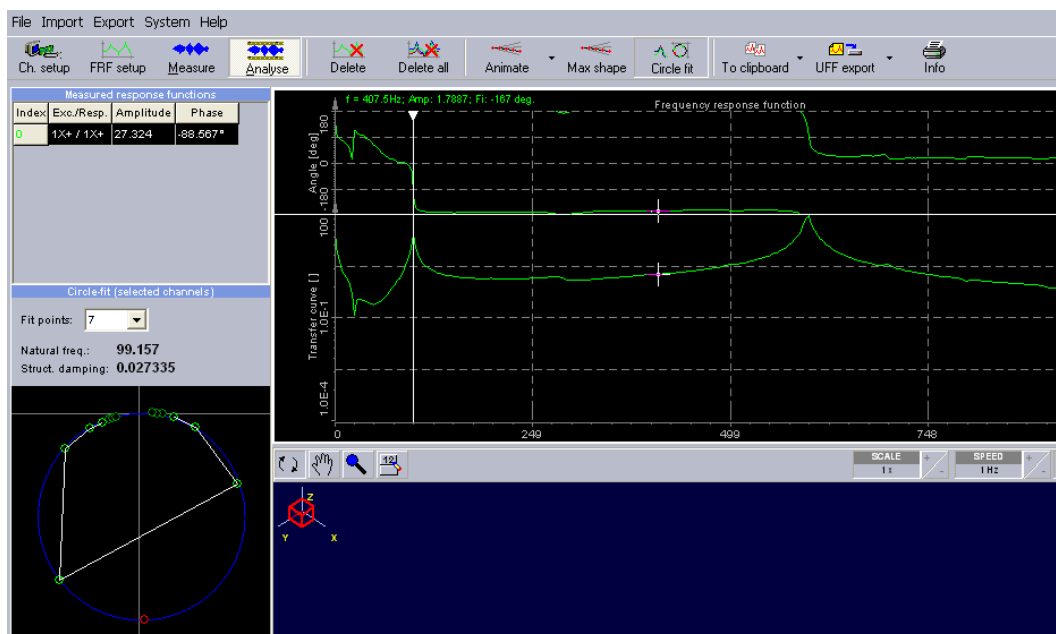Crack depth 5 mm

Figure 13: Damping loss factor of a U-shaped cracked case; Crack location 200 mm;
Crack depth 5 mm

6. Results and Discussion

In this study, the stiffness of a cracked cantilever beam that had different crack geometries, crack locations, and crack depths was investigated by theoretical and numerical methods. The bending stiffness (*K*) of the EN 42 beam is 65756.8 *N/m*. The torsional and bending stiffness of various cracked cases is presented in Table 3 and Table 4. The numerical resonant amplitudes for various cracked cases are presented in Table 5. Table 6 shows the numerical and experimental damping loss factors of various cracked cases of beams.

Crack location (mm)	Crack depth (mm)	Torsional Stiffness (K_T) N-m/rad	Bending stiffness (k) N/m
100	5	1438120	62881.59
	10	269764.1	52869.5
	15	51631.3	28922.09
200	5	2556658	64107.95
	10	479580.6	57827.84
	15	91788.99	38311.09
300	5	5752480	65013.63
	10	1079056	61979.8
	15	206525.2	49876.37
400	5	23009920	65569.42
	10	4316225	64770.04
	15	826100.9	60908.54

Table 3: Torsional stiffness and bending stiffness of EN 42 open-edged cracked cantilever beam

Crack location (mm)	Crack Depth (mm)	Methods	Bending stiffness (k) N/m	
			V-shaped crack	U-shaped crack
100	5	Numerical method	63291.14	63000
		Theoretical method	62881.59	62881.59
		Percent error	2.605229	0.187952
	10	Numerical method	53705.69	52576.23
		Theoretical method	52869.5	52869.5
		Percent error	3.497195	-0.5578
	15	Numerical method	30674.85	28074.11
		Theoretical method	28922.09	28922.09
		Percent error	7.572252	-3.02051
200	5	Numerical method	64432.99	64184.85
		Theoretical method	64107.95	64107.95
		Percent error	2.465414	0.11981
	10	Numerical method	58343.06	57670.12
		Theoretical method	57827.84	57827.84
		Percent error	2.836579	-0.27349
	15	Numerical method	39904.23	37735.84
		Theoretical method	38311.09	38311.09
		Percent error	5.884639	-1.52441
300	5	Numerical method	65189.05	65104.16
		Theoretical method	65013.63	65013.63
		Percent error	2.234698	0.139054
	10	Numerical method	62344.14	61957.86
		Theoretical method	61979.8	61979.8
		Percent error	2.543783	-0.03541
	15	Numerical method	51124.74	49261.08
		Theoretical method	49876.37	49876.37
		Percent error	4.364607	-1.24904
400	5	Numerical method	65703.02	65703.02
		Theoretical method	65569.42	65569.42
		Percent error	2.170239	0.203339
	10	Numerical method	64935.06	64850.84
		Theoretical method	64770.04	64770.04
		Percent error	2.220025	0.124594
	15	Numerical method	61425.06	60827.25
		Theoretical method	60908.54	60908.54
		Percent error	2.795213	0.13364

Table 4: The bending stiffness of EN 42 cracked cantilever beams

Crack location (mm)	Crack Depth (mm)	X_{res}, Resonant amplitude (m)	
		V-shaped crack	U-shaped crack
100	5	0.01411	0.01538
	10	0.008272	0.00732
	15	0.01704	0.01056
200	5	0.01067	0.01127
	10	0.03555	0.02404
	15	0.008559	0.01211
300	5	0.009191	0.009337
	10	0.01927	0.02264
	15	0.009295	0.01422
400	5	0.008398	0.008398
	10	0.009642	0.009801
	15	0.02984	0.04639

Table 5: The numerical resonant amplitude of EN 42 cracked cantilever beams

Crack location (mm)	Crack Depth (mm)	Numerical damping loss factor		% variation	Experimental damping loss factor		% variation
		V-shaped crack	U-shaped crack		V-shaped crack	U-shaped crack	
100	5	0.027994	0.025801	-8.4993	0.0277	0.0268	3.249
	10	0.056274	0.064959	13.36972	0.038	0.0391	-2.894
	15	0.047829	0.084328	43.2824	0.038	0.0377	0.789
200	5	0.036364	0.034561	-5.21647	0.0271	0.0273	-0.738
	10	0.012053	0.018032	33.15691	0.0291	0.0294	-1.030
	15	0.073198	0.054707	-33.8	0.04	0.042	-5
300	5	0.041726	0.041127	-1.45622	0.028	0.027	3.571
	10	0.02081	0.017822	-16.7604	0.0337	0.033	2.077
	15	0.052609	0.035689	-47.4087	0.0332	0.03	9.638
400	5	0.045308	0.045308	0	0.0268	0.03	-11.940
	10	0.039929	0.039333	-1.5172	0.0332	0.036	-8.433
	15	0.013639	0.00886	-53.9495	0.028	0.03	-7.142

Table 6: Numerical and Experimental Percentage variation of damping loss factor between V-shaped and U-shaped cracked cases for EN 42 cantilever beam
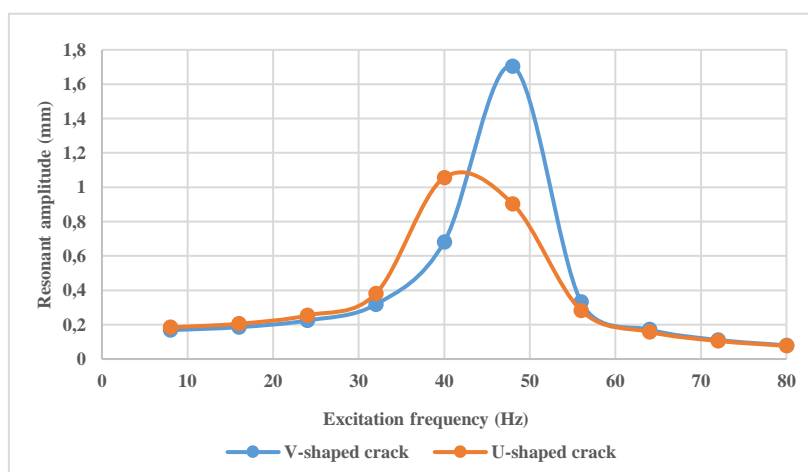

Figure 14: Variation of resonant amplitude with respect to excitation frequency; crack location 100 mm; crack depth 15 mm
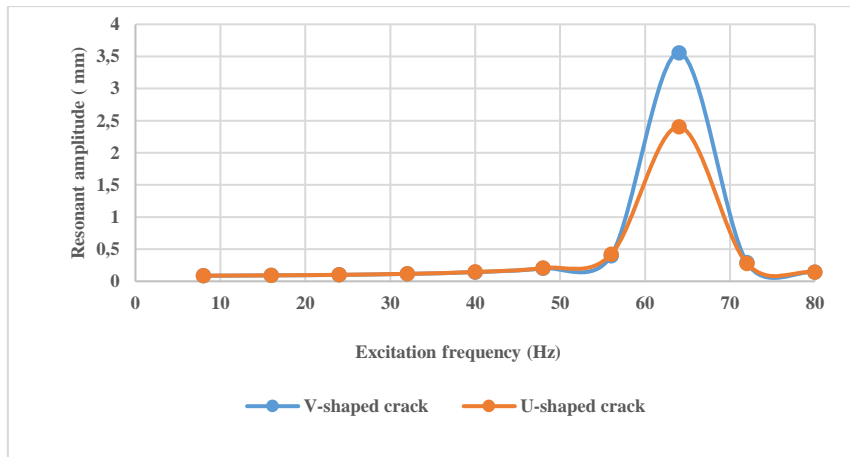
Figure 15: Variation of resonant amplitude with respect to excitation frequency; crack location 200 mm; crack depth 10 mm
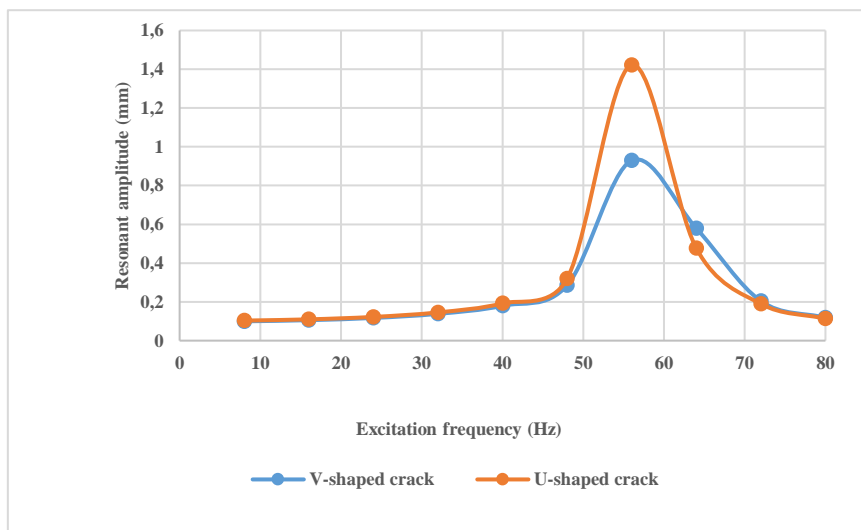

Figure 16: Variation of resonant amplitude with respect to excitation frequency; crack location 300 mm; crack depth 15 mm
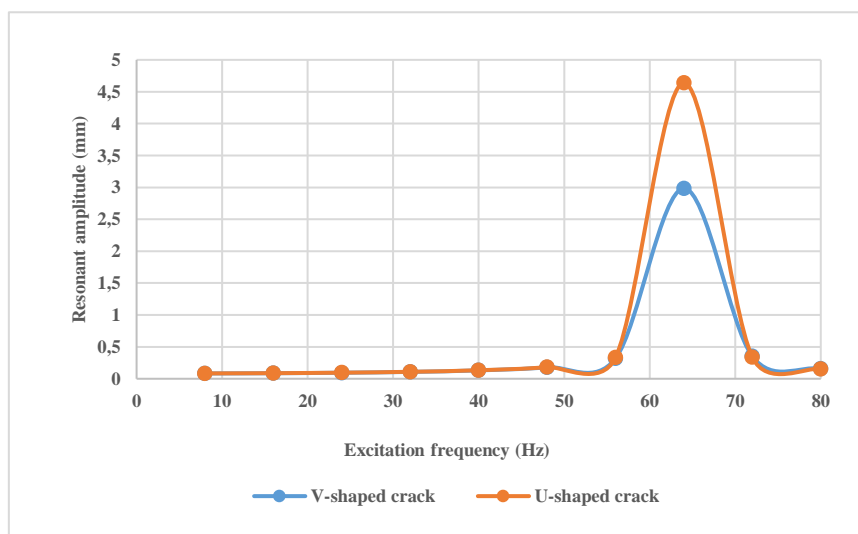

Figure 17: Variation of resonant amplitude with respect to excitation frequency; crack location 400 mm; crack depth 15 mm
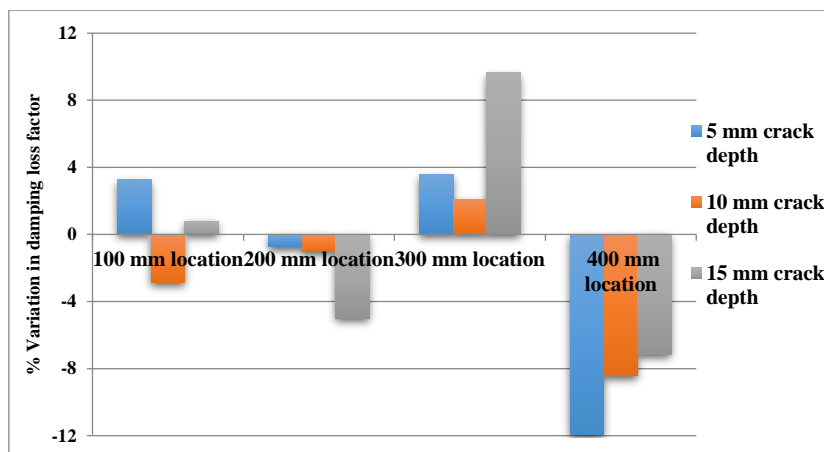
Figure 18: % Experimental variation of damping factor between V-shaped and U-shaped cracked cases for same crack configuration
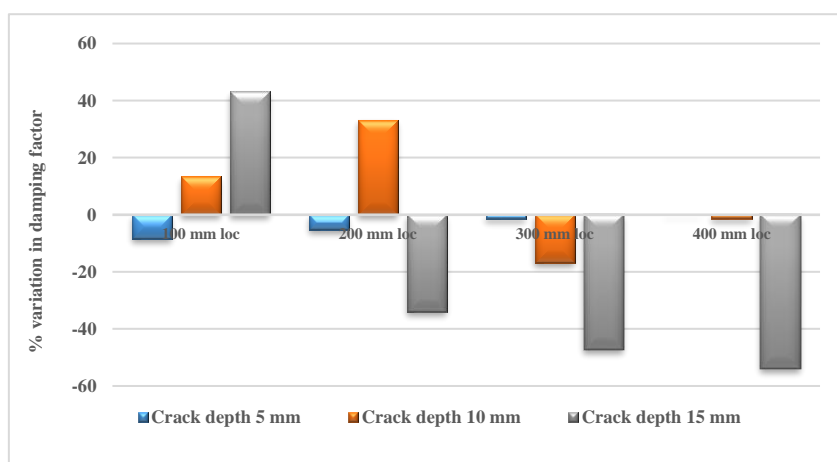

Figure 19: % Numerical variation of damping factor between V-shaped and U-shaped cracked cases for same crack configuration

Figures 14-17 show the variation in the displacement response of a cracked cantilever with respect to the excitation frequency. The V and U-shaped cracked cases of a cantilever beam give the maximum displacement response when the excitation frequency is equal to the natural frequency of the cracked beam. Figures 14-17 showed a significant difference for the resonant vibration amplitude between the U and V-shaped cracked cases for the same configurations, i.e., crack depth and crack location. It means that a cracked cantilever beam's dynamic response, i.e., resonant amplitude, is highly sensitive to the crack geometries for the same configurations. Figures 18-19 show the experimental and numerical percentage variation of damping loss factor between the V and U-shaped cracked cases for same the configurations. From Figure 18, experimentally, it was found that the percentage variation for the damping loss factor between the V and U-shaped crack models was varied from 0 to 9.638 on the positive side and from 0 to -11.94 on the negative sides. It means that the variation for the damping loss factors corresponding to change in the crack geometries (V-shaped and U-shaped cracks) shows a minor effect on the damping loss factor. On the other hand, from Figure 19 numerically, it was revealed that the percentage variation for the damping loss factor between the V and U-shaped crack models was noted to be varying from 0 to 43.2824 on the positive side and from 0 to -53.9495 on the negative sides. It implies that the variation between the damping loss factors corresponding to the crack geometries plays a key role.

Therefore, it was clearly understood that the numerical damping loss factor results were susceptible to the changes in the crack geometries.

From the previous numerical study, it was found that stiffness (Khalkar and Ramachandran 2018a), natural frequency (Khalkar and Ramachandran 2019), and mode shapes (Khalkar and Logesh 2020) are less sensitive to the change in crack geometries. It indicates that the numerical damping model needs some correction to give valid results for the damping parameter. An attempt has been made to use the effect of damping loss factor as a basic criterion for crack detection in the structures. Hence, through this study, it is clear that the numerical-based crack detection method using damping loss factor cannot satisfactorily predict the location and depth of the crack in structures irrespective of the crack geometries, i.e., V-shaped and U-shaped open edge cracks.

7. Conclusions

Numerical and theoretical methods were used to analyze the steel cracked beam's free vibrations with various crack locations, crack depths and crack geometries. The following findings can be made from a free vibration investigation of a cracked cantilever beam:

- Numerical damping loss factors of a cracked cantilever beam are susceptible to the change of crack geometries than the other modal parameters like natural frequency, stiffness and mode shapes. The inconsistencies of damping in portraying damage are different from the natural frequencies, stiffness, and mode shapes, need to be further clarified.
- Experimental damping loss factors of a cracked cantilever beam are less sensitive to the change of crack geometries than numerical damping loss factors in beams for the same configurations.
- When damping is used to describe the damage, clarifying the damping mechanism and creating a valid damping model are key components to obtain the reliable results.

References

Bayissa, W. L., N. Haritos, and S. Thelandersson. 2008. "Vibration-based structural damage identification using wavelet transform". *Mechanical Systems and Signal Processing* 22, no. 5: 1194-215. https://doi.org/10.1016/j.ymssp.2007.11.001.

Curadelli, R. O., J. D. Riera, D. Ambrosini, and M. G. Amani. 2008. "Damage detection by means of structural damping identification". *Engineering Structures* 30, no. 12: 3497-504. https://doi.org/10.1016/j.engstruct.2008.05.024.

Frizzarin, M., M. Q. Feng, P. Franchetti, S. Soyoz, and C. Modena. 2010. "Damage detection based on damping analysis of ambient vibration data". *Structural Control and Health Monitoring* 17, no. 4: 368-85. https://doi.org/10.1002/stc.296.

Kawiecki, G. 2001. "Modal damping measurement for damage detection". *Smart Materials and Structures* 10, no. 3: 466-71. https://doi.org/10.1088/0964-1726/10/3/307.

Khalkar, V., and S. Ramachandran. 2017a. "Paradigm for natural frequency of an un-cracked cantilever beam and its application to cracked beam". *ARPN Journal of Engineering and Applied Sciences* 12, no. 6: 1714-29.

———. 2017b. "Vibration analysis of a cantilever beam for oblique cracks". *ARPN Journal of Engineering and Applied Sciences* 12, no. 4: 1144-51.

———. 2018a. "The effect of crack geometry on stiffness of spring steel cantilever beam". *Journal of Low Frequency Noise Vibration and Active Control* 37, no. 4: 762-73. https://doi.org/10.1177/1461348418765959.

———. 2018b. "Study of free undamped and damped vibrations of a cracked cantilever beam". *Journal of Engineering Science and Technology* 13, no. 2: 449-62.

———. 2019. "The effect of crack geometry on non-destructive fault detection of EN 8 and EN 47 cracked cantilever beam". *Noise and Vibration Worldwide* 50, no. 3: 92-100. https://doi.org/10.1177/0957456519834537.

Khalkar, V., and K. Logesh. 2020. "The effect of crack geometry on mode shapes of a cracked cantilever beam". *Australian Journal of Mechanical Engineering*. Article in Press. https://doi.org/10.1080/14484846.2020.1766349.

Kyriazoglou, C., B. H. Le Page, and F. J. Guild. 2004. "Vibration damping for crack detection in composite laminates". *Composites Part A: Applied Science and Manufacturing* 35, no. 7-8: 945-53. https://doi.org/10.1016/j.compositesa.2004.01.003.

Orhan, S., M. Lüy, M. H. Dirikolu, and G. M. Zorlu. 2016. "The effect of crack geometry on the nondestructive fault detection in a composite beam". *International Journal of Acoustics and Vibrations* 21, no. 3: 271-73. https://doi.org/10.20855/ijav.2016.21.3420.

Razak, H. A., and F. C. Choi. 2001. "The effect of corrosion on the natural frequency and modal damping of reinforced concrete beams". *Engineering Structures* 23, no. 9: 1126-33. https://doi.org/10.1016/S0141-0296(01)00005-0.

Thomson, W., and M. D. Dahleh. 1998. *Theory of Vibration with applications*. 5th ed. Prentice-Hall.

Nomenclature

L	Length of the beam, *m*
L_1	Distance of the crack from cantilevered end, *m*
B	Width of the beam, *m*
a	Depth of crack, *m*
ζ	Damping loss factor of a cracked beam
c	Damping coefficient, *N-sec/m*
Φ'	Phase angle, degree
c_c	Critical damping coefficient, *N-sec/m*
K_T	Torsional stiffness of the cracked beam, *N-m/rad*
H	Depth of the beam, *m*
k	Open-edged crack beam stiffness, *N/m*
K_I	Intact beam stiffness, *N/m*
m_{eff}	Effective mass of the cracked cantilever beam, *kg*

m	Total mass of the cracked cantilever beam, kg
f_n	Natural frequency of cracked beam, $Hertz$
μ	Poisson's ratio
E	Young's modulus, N/m^2
ρ	Mass density of the beam, kg/m^3
M	Total mass of the intact cantilever beam, kg
x_{res}	Resonant amplitude, m

Abbreviation

SPC	Specific Damping Coefficient
EN	Euro Norm
FEA	Finite Element Analysis
FBD	Free Body Diagram
FRF	Frequency Response Function
FFT	Fast Fourier Transform